THE JOURNAL OF PHYSICAL CHEMISTRY A

Article

pubs.acs.org/JPCA

The α-Effect in Gas-Phase S_N2 Reactions of Microsolvated Anions: Methanol as a Solvent

Ditte L. Thomsen,[†,‡] Jennifer N. Reece,[‡] Charles M. Nichols,[‡] Steen Hammerum,[†] and Veronica M. Bierbaum*[,‡]

[†]Department of Chemistry, University of Copenhagen, Universitetsparken 5, DK-2100 Copenhagen, Denmark

[‡]Department of Chemistry and Biochemistry, University of Colorado, 215 UCB, Boulder, Colorado 80309, United States

ABSTRACT: The α-effect, an enhanced reactivity of nucleophiles with a lone-pair adjacent to the reaction center, has been studied in solution for several decades. The gas-phase α-effect has recently been documented in studies of S_N2 reactions as well as in competing reactions for both bare and microhydrated anions. In the present work we extend our studies of the significance of microsolvation on the α-effect, employing methanol as the solvent, in the expectation that the greater stability of the methanol cluster relative to the water cluster will lower the reactivity and thereby allow studies over a wider efficiency range. We compare the gas-phase reactivity of the microsolvated α-nucleophile $HOO^-(CH_3OH)$ to that of microsolvated normal alkoxy nucleophiles, $RO^-(CH_3OH)$ in reactions with CH_3Cl and CH_3Br. The results reveal enhanced reactivity of $HOO^-(CH_3OH)$ toward both methyl halides relative to the normal nucleophiles, and clearly demonstrate the presence of an α-effect for the microsolvated α-nucleophile. The highly exothermic reactions with methyl bromide result in a smaller Brønsted β_{nuc} value than observed for methyl chloride, and the α-effect in turn influences the reactions with methyl chloride more than with methyl bromide. Computational investigations reveal that reactions with methyl bromide proceed through earlier transition states with less advanced bond formation compared to the related reactions of methyl chloride. In addition, solvent interactions for HOO^- are quite different from those with the normal nucleophiles at the transition state, indicating that differential solvation may well contribute to the α-effect. The greater thermodynamic and kinetic stability of the anion-methanol clusters relative to the anion-water clusters accounts well for the differences in the influence of solvation with the two protic polar solvents.

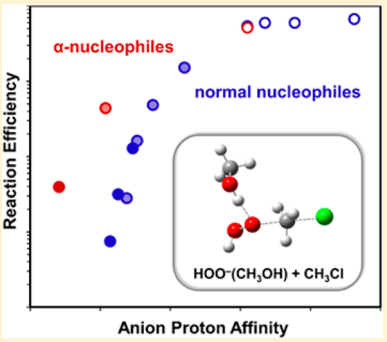

INTRODUCTION

Nucleophiles that possess a lone pair of electrons adjacent to the attacking center are known as α-nucleophiles. The term covers both ionic nucleophiles such as the hydrogen peroxide and hypochlorite anions, and neutral nucleophiles such as hydrazine and hydroxylamine. In solution, α-nucleophiles are known to display enhanced reactivity relative to normal nucleophiles of similar basicity, and the term α-effect[1] has been used to describe this modified reactivity which can be assessed with Brønsted type correlations. The effect has been observed in several different types of reactions including S_N2 reactions.[2−7] The magnitude of the α-effect for reactions with specific substrates can be determined as the ratio of rate constants for the reactions of an α-nucleophile (k_α) and a normal nucleophile (k_{normal}) of similar basicity.[8] α-Effects have been reported for numerous reactions in such diverse solvents as H_2O, dimethylsulfoxide (DMSO), and CH_3CN.[9] This has led to an active controversy about whether the α-effect is controlled by inherent properties of the α-nucleophile or by external solvent effects.

Gas-phase studies provide a vital means to explore the intrinsic nature of the α-effect. Recently, the presence of an intrinsic component of the α-effect in S_N2 reactions was demonstrated by comparing the gas-phase reactivity of HOO^- to that of the normal nucleophiles HO^-, CH_3O^-, $C_2H_5O^-$, and i-$C_3H_7O^-$ in reactions with methyl fluoride, anisole, and fluoroanisole.[10] Furthermore, a gas-phase α-effect has been shown to affect reactions of HOO^- with methyl formate[11,12] and dimethyl methylphosphonate,[13] and theoretical studies support the premise that the α-effect has a component that can be attributed to intrinsic properties of the nucleophile.[14−19]

The influence of solvent on the α-effect still remains intriguing. It is possible in gas-phase ion−molecule studies to investigate reactions in an environment with a controlled number of solvent molecules, known as microsolvation. In a recent paper[20] describing S_N2 reactions of microsolvated anions (HOO^-, HO^-, CH_3O^-, $C_2H_5O^-$, and i-$C_3H_7O^-$) with methyl chloride, we demonstrated how associating the anions with a single water molecule uncovered the presence of an α-effect otherwise not apparent for the reactions of the unsolvated anions.[21] In the absence of solvation large reaction efficiencies mask the α-effect,[22] but the association of a single water

Special Issue: A. W. Castleman, Jr. Festschrift

Received: August 1, 2013
Revised: October 9, 2013
Published: October 11, 2013

dx.doi.org/10.1021/jp407698a | J. Phys. Chem. A 2014, 118, 8060−8066

Table 1. Thermodynamic Data, Kinetic Data, and Product Distributions for the S_N2 Reactions of Microsolvated Anions with Methyl Chloride: $Nu^-(CH_3OH) + CH_3Cl$

	thermodynamic data[a]			kinetic data[b]		product distribution[c]	
	PA	ΔH_{solv}	ΔH_r	k_{exp} ($\times 10^{-11}$)	eff	Cl^-	$Cl^-(CH_3OH)$
$CH_3O^-(CH_3OH)$	1508	−112	−91/−157	2.6 ± 0.1	0.013	0.68	0.32
$C_2H_5O^-(CH_3OH)$	1500	−104	−83/−150	0.61 ± 0.04	0.0032	0.52	0.29[d]
i-$C_3H_7O^-(CH_3OH)$	1496	−100	−71/−138	0.14 ± 0.01	0.00075	e	e
$HOO^-(CH_3OH)$	1466	−122	−64/−130	0.79 ± 0.06	0.0039	0.67	0.33

[a]Thermodynamic data in units of kJ/mol calculated using G3; proton affinity (PA) of the microsolvated anion; solvation enthalpy (ΔH_{solv}); reaction enthalpy (ΔH_r) displayed for Cl^- and clustered $Cl^-(CH_3OH)$ products, respectively ($Cl^-/Cl^-(CH_3OH)$). [b]Overall rate constant (k_{exp}) in units of cm^3 $molecule^{-1}$ s^{-1}. Error bars represent one standard deviation, absolute uncertainty is ±30%. Reaction efficiency (eff) is the ratio of the overall rate constant (k_{exp}) to the collision rate constant (k_{col}). [c]Absolute uncertainty is ±50%. [d]Additional 0.19 $Cl^-(C_2H_5OH)$ formation. [e]Because of the low reactivity, a product distribution could not be determined.

molecule causes a significant decrease in reaction efficiency, and allows detection of an α-effect.[20] In the present work we expand the study to anions clustered with a single methanol molecule, as previous investigations of S_N2 reactions of methanol-microsolvated nucleophiles have demonstrated a more pronounced attenuation of the reaction efficiency compared to water solvation.[23,24] This is a consequence of the greater solvation energy for anions with methanol relative to water, causing greater thermodynamic and kinetic stability of these cluster ions. Therefore, methanol-microsolvation makes it possible to study the α-effect over a much wider efficiency range than can be achieved with water-solvation. Furthermore, complementing the reactions with methyl chloride, methanol solvation allows us to investigate the reaction efficiencies with the more reactive methyl bromide.

The α-nucleophile investigated in this study is the microsolvated hydrogen peroxide anion, $HOO^-(CH_3OH)$. We report overall rate constants and reaction efficiencies along with product distributions for the gas-phase reactions of HOO^-, CH_3O^-, $C_2H_5O^-$, and i-$C_3H_7O^-$ with methyl chloride and methyl bromide in the presence of a single methanol molecule. The α-nucleophilicity of the microsolvated $HOO^-(CH_3OH)$ is examined by comparing the reaction efficiency to that of the microsolvated normal nucleophiles. Reactions of an $HO^-(CH_3OH)$ cluster cannot be studied, since the proton affinity of HO^- (1633 kJ/mol)[25] is larger than that of CH_3O^- (1598 kJ/mol),[25] and any attempt to form the desired $HO^-(CH_3OH)$ cluster would instead lead to formation of a water-solvated methoxy anion, $CH_3O^-(H_2O)$.

EXPERIMENTAL METHODS

The experiments were carried out with a flowing afterglow-selected ion flow tube (FA-SIFT) mass spectrometer.[26,27] The instrument consists of four sections: an ion source flow tube, an ion selection region, a reaction flow tube, and a detection region. All anions were generated by proton abstraction of the corresponding neutrals by NH_2^-, which was prepared by electron ionization (70 eV) of ammonia. The microsolvated ions were prepared by introducing methanol slightly downstream of the ionizer and then mass selected using a quadrupole mass filter prior to injection into the reaction flow tube.

Reaction rate constants were obtained by monitoring the ion signal as a function of reaction distance. All reported reaction rate constants and product distributions represent the average of at least three individual measurements. A systematic error in the experimental rate constants was discovered by intercomparison of current values to previous measurements and those of other laboratories; the origin of the problem was related to high helium flow through the inner annulus of the Venturi inlet, resulting in turbulence. A correction factor of 1.18 was determined by comparing rate constants measured before and after correction of the problem; this factor has been applied to the reported rate constants. Reaction efficiencies are obtained as the ratio between the experimental rate constant (k_{exp}) and the collision rate constant (k_{col}), with k_{col} calculated from parametrized trajectory collision rate theory.[28] To exclude any secondary reaction products, product distributions are determined by extrapolating the product yields to zero reaction time. As a result of collision-induced dissociation upon injection of the microsolvated ion into the reaction flow tube the bare ion is always present, and the product distributions of the microsolvated anions are corrected for reaction of the bare ion. Mass discrimination was minimized. Absolute uncertainties are ±30% for the rate constants and ±50% for the product distributions. Helium buffer gas (He, Airgas, 99.995%) was purified by passage through a molecular sieve trap immersed in liquid nitrogen. All reagents were obtained from commercial sources and used without further purification: methyl chloride (CH_3Cl, Matheson, 99.5%); methyl bromide (CH_3Br, Matheson, ≥99.5%); hydrogen peroxide (H_2O_2, Sigma-Aldrich, 50 wt.% solution in water); methanol (CH_3OH, Honeywell B&J, 99.9%); ethanol (C_2H_5OH, Decon Laboratories, 200 proof); isopropanol (i-C_3H_7OH, Fisher Scientific, 99.9%), ammonia (NH_3, Airgas, 99.9995%).

COMPUTATIONAL METHODS

Reactant, transition state and products structures were optimized as stationary points on the MP2/6-311++G(d,p) potential energy surface. Harmonic vibrational frequencies were obtained at the same level and used to verify the nature of the stationary points as minima and first order saddle points, respectively. Thermochemical properties were calculated using a modified version of the composite G3 method in which diffuse basis functions are included to allow a better description of the anions as previously described.[20] All calculations were carried out with the Gaussian 09 program.[29] Proton affinities (PA) of the microsolvated nucleophiles correspond to the calculated reaction enthalpy at 298 K:

$$Nu^-(H_2O) + H^+ \rightarrow NuH(H_2O) \quad (1)$$

RESULTS AND DISCUSSION

Reaction Efficiencies. The rate constants and reaction efficiencies measured for the S_N2 reactions of microsolvated anions with methyl chloride and methyl bromide are displayed in Tables 1 and 2, together with the calculated reaction

dx.doi.org/10.1021/jp407698a | J. Phys. Chem. A 2014, 118, 8060−8066

Table 2. Thermodynamic Data, Kinetic Data, and Product Distributions for the S_N2 Reactions of Microsolvated Anions with Methyl Bromide: $Nu^-(CH_3OH) + CH_3Br$

	thermodynamic data[a]			kinetic data[b]		product distribution[c]	
	PA	ΔH_{solv}	ΔH_r	k_{exp} ($\times 10^{-11}$)	eff	Br^-	$Br^-(CH_3OH)$
$CH_3O^-(CH_3OH)$	1508	−112	−123/−181	57 ± 2	0.33	0.95	0.05
$C_2H_5O^-(CH_3OH)$	1500	−104	−115/−174	38 ± 2	0.23	0.89	0.08[d]
i-$C_3H_7O^-(CH_3OH)$	1496	−100	−103/−162	20 ± 1	0.13	0.91	0.09
$HOO^-(CH_3OH)$	1466	−122	−97/−154	45 ± 1	0.26	0.92	0.08

[a]Thermodynamic data in units of kJ/mol calculated using G3; proton affinity (PA) of the microsolvated anion; solvation enthalpy (ΔH_{solv}); reaction enthalpy (ΔH_r) displayed for Br^- and clustered $Br^-(CH_3OH)$ products, respectively ($Br^-/Br^-(CH_3OH)$). [b]Overall rate constant (k_{exp}) in units of cm^3 $molecule^{-1}$ s^{-1}. Error bars represent one standard deviation, absolute uncertainty is ±30%. Reaction efficiency (eff) is the ratio of the overall rate constant (k_{exp}) to the collision rate constant (k_{col}). [c]Absolute uncertainty is ±50%. [d]Additional 0.04 $Br^-(C_2H_5OH)$ formation.

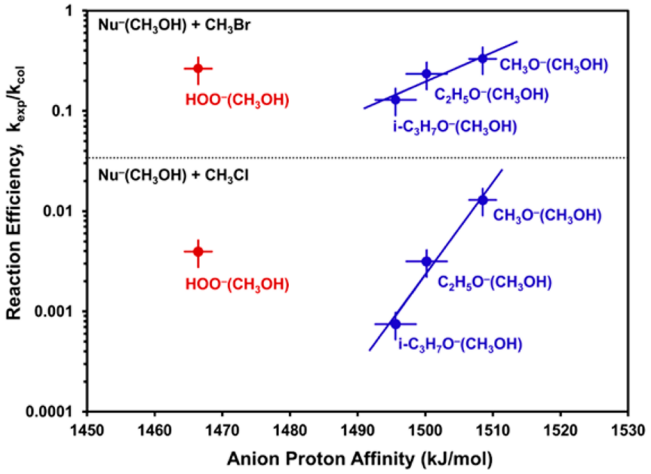

Figure 1. Reaction Efficiency (k_{exp}/k_{col}) vs Anion Proton Affinity (PA) for the S_N2 reactions of microsolvated anions with methyl bromide (top) and methyl chloride (bottom). Normal nucleophiles are displayed in blue and α-nucleophiles in red. The linear trend lines are fits to the normal nucleophile data sets. The reaction efficiency is the ratio of the overall rate constant (k_{exp}) compared to the collision rate constant (k_{col}). The anion proton affinity is calculated using G3. The vertical error bars represent the absolute uncertainty of ±30%. The horizontal error bars represent the experimental uncertainty in the proton affinity of the bare ion, against which the computed PAs are benchmarked.

thermochemistry and proton affinities of the microsolvated nucleophiles. Figure 1 shows a Brønsted type plot of the reaction efficiency versus the proton affinity of the microsolvated anions. Efficiencies associated with the reaction of methyl bromide appear in the upper panel and of methyl chloride in the lower panel. The higher reaction exothermicities of the methyl bromide reactions are reflected in large reaction efficiencies. Reactions of these two methyl halides provide access to the α-effect in two very different efficiency ranges. The results indicate that the $HOO^-(CH_3OH)$ cluster exhibits a pronounced α-effect in the S_N2 reaction with both methyl chloride and methyl bromide, since the reactions of this cluster show a significant deviation from the rate-energy relationship found for the normal microsolvated nucleophiles.

Product Distributions. Gas-phase S_N2 reactions of microsolvated nucleophiles with methyl halides can produce the bare halide ion (2a) as well as the microsolvated product ion (2b):

$$Nu^-(CH_3OH) + CH_3X \rightarrow NuCH_3 + X^- + CH_3OH \quad (2a)$$

$$\rightarrow NuCH_3 + X^-(CH_3OH) \quad (2b)$$

The product distributions for formation of X^- and $X^-(CH_3OH)$ for the various microsolvated nucleophiles are shown in Tables 1 and 2 for reaction with methyl chloride and methyl bromide, respectively. Formation of the clustered product is the more exothermic process, and could well be expected to dominate; nonetheless, formation of the unsolvated halide anion dominates over the microsolvated ion in both reactions. In the more exothermic reactions of methyl bromide we observe almost exclusively formation of Br^-, while the microsolvated $Br^-(CH_3OH)$ in all cases constitutes less than 10% of the ionic products. When methyl chloride is the substrate we observe about 30% formation of the microsolvated $Cl^-(CH_3OH)$ product ion. Previous investigations of gas-phase S_N2 reactions involving microsolvated nucleophiles and methyl halides have shown similar product distributions, in which formation of the nonsolvated product dominates.[20,23,30−32] Several factors may contribute to the preferred formation of the thermodynamically less favorable nonsolvated product, and explanations suggesting steric properties,[33] product dynamics in a postreaction complex,[34] as well as redistribution of excess reaction energy,[35] have been proposed.

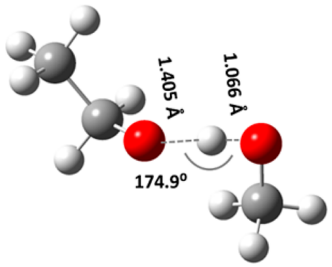

Figure 2. Structure of the microsolvated $C_2H_5O^-(CH_3OH)$ anion optimized at the MP2/6-311++G(d,p) level of theory.

The reactions of the microsolvated ethoxy anion, $C_2H_5O^-(CH_3OH)$ (Figure 2) exhibit an additional product channel. Besides formation of the bare X^- ion and the $X^-(CH_3OH)$ cluster we observe formation of an ethanol microsolvated $X^-(C_2H_5OH)$ cluster, which suggests that the microsolvated ethoxy anion may react as $CH_3O^-(C_2H_5OH)$ as well:

$$CH_3O^-(C_2H_5OH) + CH_3X \rightarrow CH_3OCH_3 + X^-(C_2H_5OH) \quad (3)$$

When methyl chloride is the substrate we observe 19% formation of the $Cl^-(C_2H_5OH)$ cluster, and with methyl bromide the $Br^-(C_2H_5OH)$ cluster constitutes 4% of the product distribution. The proton affinity of CH_3O^- (1598 kJ/

dx.doi.org/10.1021/jp407698a | J. Phys. Chem. A 2014, 118, 8060−8066

mol)[25] is larger than that of $C_2H_5O^-$ (1585 kJ/mol)[25] but only by 13 kJ/mol. Apparently, this difference is small enough to allow the cluster ion to react at either oxygen center. The calculated enthalpy of the transition state corresponding to $CH_3O^-(C_2H_5OH)$ attack is only 5 kJ/mol above that of the transition state of $C_2H_5O^-(CH_3OH)$ attack. This is consistent with the experimental results, supporting that both reactions occur with similar reaction efficiency. However, reaction of the microsolvated propoxy anion does not result in any formation of a X^-(i-C_3H_7OH) product. The proton affinity difference in the i-$C_3H_7O^-(CH_3OH)$ cluster is larger (22 kJ/mol), allowing the cluster to react exclusively as i-$C_3H_7O^-(CH_3OH)$.

It was recently shown that the structure of the $HOO^-(H_2O)$ cluster resembles HO^-(HOOH), but that HOO^- is the active nucleophile when the cluster reacts.[12,20] Our computational results show that the $HOO^-(CH_3OH)$ cluster (Figure 3)

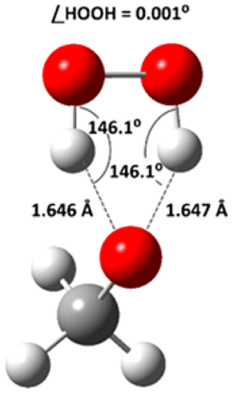

Figure 3. Structure of the microsolvated $HOO^-(CH_3OH)$ anion optimized at the MP2/6-311++G(d,p) level of theory.

possesses a similar structure, resembling CH_3O^-(HOOH). Reactions of the microsolvated ion with both methyl halides result in formation of the bare X^- ion and the $X^-(CH_3OH)$ cluster, but not of any X^-(HOOH) species. This implies that HOO^- is the reactive nucleophile, which in turn suggests that the enhanced reactivity of $HOO^-(CH_3OH)$ can indeed be ascribed to the α-nucleophilic character of the HOO^- anion. Reaction paths for reactions of $HOO^-(CH_3OH)$ and CH_3O^-(HOOH) with methyl chloride and methyl bromide were examined computationally. The optimized transition state structures are displayed in Figure 4 together with transition state enthalpies. The enthalpy of the transition states

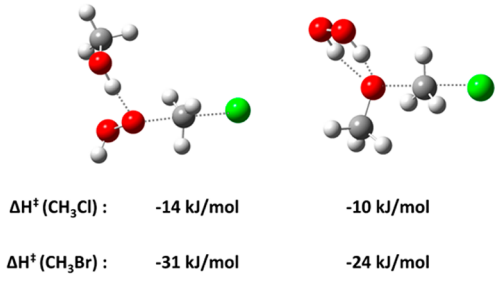

Figure 4. Transition state structures for the S_N2 reaction of a methanol-microsolvated HOO^- with methyl chloride corresponding to attack by $HOO^-(CH_3OH)$ (left) and CH_3O^-(HOOH) (right) calculated using MP2/6-311++G(d,p). Transition state enthalpies corresponding to reaction with methyl chloride and methyl bromide, respectively, calculated using G3.

corresponding to $HOO^-(CH_3OH)$ attack are calculated to be only 4 and 7 kJ/mol below that of the transition states corresponding to CH_3O^-(HOOH) attack, suggesting a small preference for HOO^- attack.

As noted by a reviewer, the Brønsted plot in Figure 1 includes the reaction efficiency of the reactive form, $HOO^-(CH_3OH)$, versus the anion proton affinity of the stable form of the reactant ion, CH_3O^-(HOOH); we believe that this correctly reflects the actual reaction process. However, if the proton affinity of the $HOO^-(CH_3OH)$ cluster is instead assumed to be similar to that of i-$PrO^-(CH_3OH)$, because of the similar basicities of the bare anions, an α-effect is still evident, albeit significantly smaller.

Transition State Structures. In conventional S_N2 reactions the nucleophile attacks the methyl halide opposite to the leaving group, forming a trigonal bipyramidal transition state. The calculated transition state structures suggest that when the microsolvated nucleophile reacts, the hydroxyl hydrogen of the methanol molecule points toward the nucleophilic center (Figure 5). The distance between the

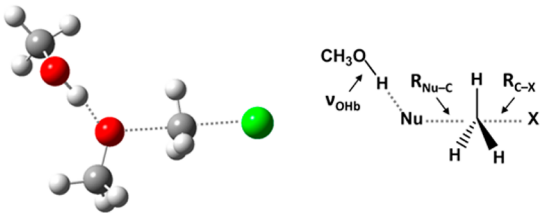

Figure 5. Transition state structure for the S_N2 reaction of a methanol-microsolvated CH_3O^- with methyl chloride. Calculated bond lengths R_{Nu-C} and R_{C-X}, as well as the red shift of the vibrational frequency of the hydrogen bonded OH stretch, $\Delta\nu_{OHb}$, are found in Table 3 for all nucleophiles examined.

nucleophile oxygen and the carbon center (R_{Nu-C}) and between the leaving group X^- and the carbon center (R_{C-X}) are displayed in Table 3. The transition state bond lengths vary only little among the different nucleophiles, although the $HOO^-(CH_3OH)$ cluster exhibits a slightly tighter transition state, in which bond formation is more advanced. Comparing the structural features when methyl chloride and methyl bromide react, we see that the less exothermic methyl chloride reaction proceeds by way of a later transition state with more pronounced Nu–C bond formation. A direct relationship between the magnitude of the α-effect and the extent of bond formation in the transition state has previously been suggested for condensed-phase reactions of other systems.[3] Taking the magnitude of the α-effect to be expressed as a positive deviation from the Brønsted-plot in Figure 1, we obtain a larger α-effect for the reaction with methyl chloride, consistent with bond formation being more advanced. Also the Brønsted β_{nuc} parameter, which is the slope of a Brønsted plot, is known to be directly related to the extent of bond formation in the transition state, and the α-effect is in turn directly related to the magnitude of the β_{nuc} value.[3] The larger slope of the methyl chloride plot (Figure 1, lower panel) is thus consistent with a later transition state and a more pronounced α-effect.

The interactions involving the solvent molecule in the transition states are reflected in the red shift ($\Delta\nu_{OHb}$) of the hydrogen bonded methanol OH stretch (Table 3). It is well established that the red shift of an OH-stretching frequency is a measure of the strength of the hydrogen bond, as a larger red

dx.doi.org/10.1021/jp407698a | J. Phys. Chem. A 2014, 118, 8060–8066

Table 3. Calculated Bond Lengths and OH_b Red Shifts for the Transition States of the S_N2 Reactions of Microsolvated Anions with Methyl Chloride and Methyl Bromide: $Nu^-(CH_3OH) + CH_3X$

	CH_3Cl			CH_3Br		
	R_{Nu-C}[a]	R_{C-Cl}[a]	$\Delta\nu_{OHb}$[b]	R_{Nu-C}[a]	R_{C-Br}[a]	$\Delta\nu_{OHb}$[b]
$CH_3O^-(CH_3OH)$	2.036	2.138	1009	2.105	2.250	1073
$C_2H_5O^-(CH_3OH)$	2.020	2.158	969	2.098	2.262	1042
i-$C_3H_7O^-(CH_3OH)$	2.020	2.161	940	2.084	2.296	997
$HOO^-(CH_3OH)$	2.016	2.145	875	2.082	2.261	937

[a]Geometries are optimized and vibrational frequencies calculated at the MP2/6-311++G(d,p) level of theory; transition state bond lengths in units of Å. [b]Red shift ($\Delta\nu_{OHb}$) in units of cm^{-1}. The red shifts of the bonded OH stretching frequency ($\Delta\nu_{OHb}$) are calculated relative to the frequency of the OH stretch (ν_{OHf}) in isolated methanol ($\Delta\nu_{OHb} = \nu_{OHf} - \nu_{OHb}$). Deuterated alkoxy groups were used in the frequency calculation to avoid coupling between the OH_b- and CH-stretches.

Table 4. Thermodynamic Data, Kinetic Data, and Calculated Structural Parameters for the S_N2 Reaction of Water-Microsolvated Anions with Methyl Chloride: $Nu^-(H_2O) + CH_3Cl$[a]

	PA[b]	ΔH_{solv}[b]	eff[c]	R_{Nu-C}[d]	R_{C-Cl}[d]	$\Delta\nu_{OHb}$[d]
$CH_3O^-(H_2O)$	1520	−99	0.049	2.044	2.133	986
$C_2H_5O^-(H_2O)$	1511	−92	0.016	2.030	2.151	947
i-$C_3H_7O^-(H_2O)$	1505	−89	0.003	2.026	2.157	904
$HOO^-(H_2O)$	1493	−106	0.044	2.023	2.141	820

[a]Values from ref 20. [b]Thermodynamic data in units of kJ/mol calculated using G3; proton affinity (PA) of the microsolvated anion; solvation enthalpy (ΔH_{solv}). [c]Reaction efficiency (eff) is the ratio of the overall rate constant (k_{exp}) to the collision rate constant (k_{col}). [d]Geometries are optimized and vibrational frequencies calculated at the MP2/6-311++G(d,p) level of theory; transition state bond lengths in units of Å and frequencies and red shifts in units of cm^{-1}. The red shifts of the bonded OH stretching frequency ($\Delta\nu_{OHb}$) are calculated relative to the frequency of the free OH stretch (ν_{OHf}) in the attached water molecule ($\Delta\nu_{OHb} = \nu_{OHf} - \nu_{OHb}$). Deuterated alkoxy groups were used in the frequency calculation to avoid coupling between the OH_b- and CH-stretches.

shift corresponds to a stronger hydrogen bond.[36] The calculated red shifts are slightly larger for the reactions of methyl bromide, suggesting a stronger hydrogen bond in the transition states. The reaction with methyl bromide proceeds through an earlier transition state in which Nu−C bond formation is less advanced, allowing the nucleophile to retain a slightly stronger solvent interaction in the transition state. Among the nucleophiles examined, $HOO^-(CH_3OH)$ has the weakest hydrogen bond to the methanol molecule in the transition state, even though this cluster exhibits the greatest solvation enthalpy (ΔH_{solv} Tables 1 and 2). This implies that the solvent interactions for the α-nucleophile differ from that of the normal nucleophiles, and indicates that in addition to inherent properties of the α-nucleophile, differential solvation may well contribute to the α-effect.

Comparison to Water-Microsolvation. The reactivity of unsolvated and microhydrated nucleophiles toward methyl chloride was recently examined;[20] associating the anions with a single water molecule lowered the reaction efficiency and allowed observation of an α-effect, which was not apparent for the unsolvated anions. Table 4 summarizes the results for the microhydrated anions, and Figure 6 shows Brønsted type plots of the reaction efficiencies for the reactions of methyl chloride with methanol- and water-microsolvated nucleophiles as well as with the unsolvated anions. Association of the nucleophile with methanol lowers the proton affinity more than does association with a water molecule, allowing the effect of microsolvation to be examined in a broader proton affinity range. The lowering of the proton affinity when going from water- to methanol-microsolvation is accompanied by a reduced reaction efficiency. Despite this lower efficiency, it appears from Figure 6 that the β_{nuc} parameter is similar for water- and methanol-solvation. Comparison of the structural parameters in the calculated methanol and water solvated transition states (Tables 3 and 4) reveals very similar structures with similar Nu−C bond formation and C−Cl bond breaking.

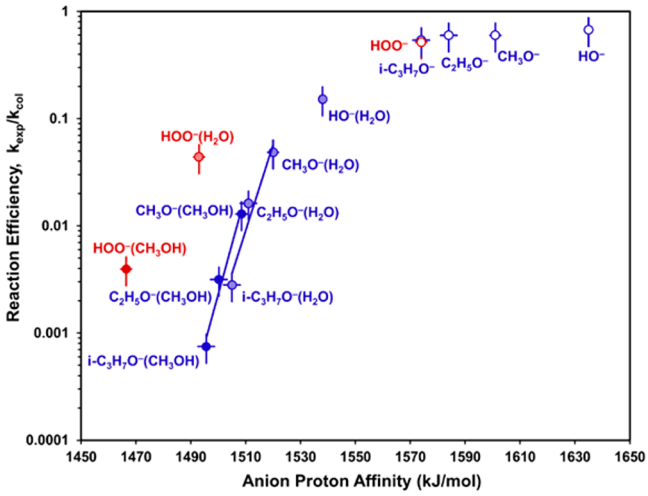

Figure 6. Reaction Efficiency (k_{exp}/k_{col}) vs Anion Proton Affinity (PA) for the S_N2 reactions of unsolvated (○), water-microsolvated (shaded circles) and methanol-microsolvated (●) anions with methyl chloride. Normal nucleophiles are displayed in blue and α-nucleophiles in red. The linear trend lines are fits to the normal nucleophile data set comprising CH_3O^-, $C_2H_5O^-$, and i-$C_3H_7O^-$ with methanol- and water-solvation, respectively. Reaction efficiencies for the unsolvated and water-solvated anions are obtained from refs 21 and 20, respectively. The reaction efficiency is the ratio of the overall rate constant (k_{exp}) compared to the collision rate constant (k_{col}). The anion proton affinity is calculated using the G3 method. The vertical error bars represent the absolute uncertainty of ±30%. The horizontal error bars represent the experimental uncertainty in the proton affinity of the bare ion, against which the computed PAs are benchmarked.

dx.doi.org/10.1021/jp407698a | J. Phys. Chem. A 2014, 118, 8060−8066

No significant differences are found regarding the nature of solvation with the two solvent molecules. Both water- and methanol-microsolvation serve to permit the observation of an α-effect in the S_N2 reactions of HOO^- that is not apparent for the unsolvated anions. The change in reactivity when the water solvent molecule is replaced by methanol is not reflected in variations in the transition state structures, in complete accordance with the very similar β_{nuc} values. As both solvents are attached to the nucleophile through a hydrogen bonding OH group, we can compare the solvent interaction in the transition states by comparing the red shift of the OH-stretching frequencies (Tables 3 and 4). The larger red shift observed for methanol indicates a slightly stronger interaction with methanol in the transition state, in accordance with larger solvation enthalpies of the $Nu^-(CH_3OH)$ cluster compared to the $Nu^-(H_2O)$ analogues. The order of decreasing solvent interaction from CH_3O^- to i-$C_3H_7O^-$ is similar for both solvents, and in both cases HOO^- displays a lower solvation interaction in the transition state than the normal nucleophiles.

CONCLUSIONS

The gas-phase S_N2 reactions of methanol-microsolvated oxygen-centered anions add further support to the suggestion that an α-effect influences the reactions of microsolvated HOO^- anions. Methanol-microsolvation allows us to investigate the reactivity with both methyl chloride and the more reactive methyl bromide, thereby enabling the investigation of the α-effect over a wider efficiency range than for water-microsolvation. Reactions of the microsolvated anions can give rise to formation of the bare X^- anion or the solvated product, $X^-(CH_3OH)$. The experimental product distribution shows preferential formation of the X^- anion even though formation of $X^-(CH_3OH)$ is the thermodynamically preferred process. The $C_2H_5O^-(CH_3OH)$ cluster has an additional product channel, in which an ethanol-microsolvated $X^-(C_2H_5OH)$ product is formed. The computational results support that reaction at the two oxygen centers in the microsolvated ethoxy cluster can occur with similar reaction efficiencies.

Computational investigations of the transition state structures suggest that the more exothermic reactions with methyl bromide proceed through earlier transition states with less advanced Nu−C bond formation compared to the related reactions of methyl chloride. This can be directly related to a smaller Brønsted β_{nuc} value obtained from the slopes of the Brønsted plot. Accordingly, we find that the α-effect influences the reactions of methyl chloride more than those involving methyl bromide.

Hydrogen bonding interactions with the methanol molecule in the transition state indicates that the α-nucleophile interacts less strongly with the solvating methanol molecule in the transition state than do the microsolvated normal nucleophiles. This result suggests that differences with regard to solvation may well contribute to the observed α-effect.

No significant differences are found in the nature of solvation between the two protic polar solvents methanol and water. Additional studies, investigating the influence of aprotic and nonpolar solvents, will contribute to our understanding of the significance of solvent interactions in the α-effect.

AUTHOR INFORMATION

Corresponding Author

*E-mail: veronica.bierbaum@colorado.edu.

Notes

The authors declare no competing financial interest.

ACKNOWLEDGMENTS

We gratefully acknowledge NSF (CHE-1012321 and CHE-1300886) for support of this research. D.L.T. thanks the Danish Chemical Society and Augustinus Foundation, C.M.N. thanks AFOSR, and J.N.R. thanks the Colorado Diversity Initiative for financial support.

REFERENCES

(1) Edwards, J. O.; Pearson, R. G. Factors Determining Nucleophilic Reactivity. *J. Am. Chem. Soc.* **1962**, *84*, 16−24.
(2) Gregory, M. J.; Bruice, T. C. α-Effect. II. Displacements on sp^3-Carbon. *J. Am. Chem. Soc.* **1967**, *89*, 4400−4402.
(3) Dixon, J. E.; Bruice, T. C. α-Effect. V. Kinetic and Thermodynamic Nature of the α-Effect for Amine Nucleophiles. *J. Am. Chem. Soc.* **1972**, *94*, 2052−2056.
(4) McIsaac, J. E., Jr.; Subbaram, L. R.; Subbaram, J.; Mulhausen, H. A.; Behrman, E. J. Nucleophilic Reactivity of Peroxy Anions. *J. Org. Chem.* **1972**, *37*, 1037−1041.
(5) Buncel, E.; Wilson, H.; Chuaqui, C. Reactivity-Selectivity Correlations and the α-Effect in S_N2 Reactions at sp^3-Carbon - Reaction of Hydrogen-Peroxide Anion with Methyl Phenyl Sulfates. *Bull. Soc. Chim. Belg.* **1982**, *91*, 420−420.
(6) Fountain, K. R.; Dunkin, T. W.; Patel, K. D. α-Effect with Substituted N-Methylbenzohydroxamates and Substituted Phenyldimethylsulfonium Salts: Toward Understanding of an Intrinsic α-Effect. *J. Org. Chem.* **1997**, *62*, 2738−2741.
(7) Fountain, K. R.; Felkerson, C. J.; Driskell, J. D.; Lamp, B. D. The α-Effect in Methyl Transfers from S-Methyldibenzothiophenium Fluoroborate to Substituted N-Methylbenzohydroxamates. *J. Org. Chem.* **2003**, *68*, 1810−1814.
(8) Hoz, S.; Buncel, E. The α-Effect - A Critical Examination of the Phenomenon and its Origin. *Isr. J. Chem.* **1985**, *26*, 313−319.
(9) Buncel, E.; Um, I. H. The α-Effect and its Modulation by Solvent. *Tetrahedron* **2004**, *60*, 7801−7825.
(10) Garver, J. M.; Gronert, S.; Bierbaum, V. M. Experimental Validation of the α-Effect in the Gas Phase. *J. Am. Chem. Soc.* **2011**, *133*, 13894−13897.
(11) Garver, J. M.; Yang, Z.; Wehres, N.; Nichols, C. M.; Worker, B. B.; Bierbaum, V. M. The α-Effect in Elimination Reactions and Competing Mechanisms in the Gas Phase. *Int. J. Mass Spectrom.* **2012**, *330*, 182−190.
(12) Thomsen, D. L.; Nichols, C. M.; Reece, J. N.; Hammerum, S.; Bierbaum, V. M. The α-Effect and Competing Mechanisms: The Gas-Phase Reactions of Microsolvated Anions with Methyl Formate. *J. Am. Soc. Mass Spectrom.* **2013**, submitted for publication.
(13) McAnoy, A. M.; Paine, M. R. L.; Blanksby, S. J. Reactions of the Hydroperoxide Anion with Dimethyl Methylphosphonate in an Ion Trap Mass Spectrometer: Evidence for a Gas-Phase α-Effect. *Org. Biomol. Chem.* **2008**, *6*, 2316−2326.
(14) Fountain, K. R. The Size of the α-Effects in Methyl Transfers Correlate with Koopmans' Theorem Ionization Potentials. *J. Phys. Org. Chem.* **2005**, *18*, 481−485.
(15) Patterson, E. V.; Fountain, K. R. On Gas-Phase α-Effects. I. The Gas-Phase Manifestation and Potential SET Character. *J. Org. Chem.* **2006**, *71*, 8121−8125.
(16) Afzal, D.; Fountain, K. R. Theoretical Investigation of Experimentally Determined α-Effects - The Role of Electronics. *Can. J. Chem.* **2011**, *89*, 1343−1354.
(17) Ren, Y.; Yamataka, H. The α-effect in Gas-Phase S_N2 Reactions Revisited. *Org. Lett.* **2006**, *8*, 119−121.
(18) Ren, Y.; Yamataka, H. The α-Effect in Gas-Phase S_N2 Reactions: Existence and the Origin of the Effect. *J. Org. Chem.* **2007**, *72*, 5660−5667.

(19) Ren, Y.; Yamataka, H. G2(+) Investigation on the α-Effect in the S_N2 Reactions at Saturated Carbon. *Chem.—Eur. J.* **2007**, *13*, 677−682.
(20) Thomsen, D. L.; Reece, J. N.; Nichols, C. M.; Hammerum, S.; Bierbaum, V. M. Investigating the α-effect in Gas-Phase S_N2 Reactions of Microsolvated Anions. *J. Am. Chem. Soc.* **2013**, *135*, 15508−15514.
(21) Villano, S. M.; Eyet, N.; Lineberger, W. C.; Bierbaum, V. M. Reactions of α-Nucleophiles with Alkyl Chlorides: Competition between S_N2 and E2 Mechanisms and the Gas-Phase α-Effect. *J. Am. Chem. Soc.* **2009**, *131*, 8227−8233.
(22) Garver, J. M.; Yang, Z.; Nichols, C. M.; Worker, B. B.; Gronert, S.; Bierbaum, V. M. Resolving the α-Effect in Gas-Phase S_N2 Reactions: A Marcus Theory Approach. *Int. J. Mass Spectrom.* **2012**, *316*, 244−250.
(23) Bohme, D. K.; Raksit, A. B. Gas-Phase Measurements of the Influence of Stepwise Solvation on the Kinetics of S_N2 Reactions of Solvated F^- with CH_3Cl and CH_3Br and of Solvated Cl^- with CH_3Br. *Can. J. Chem.* **1985**, *63*, 3007−3011.
(24) Kato, S.; Hacaloglu, J.; Davico, G. E.; DePuy, C. H.; Bierbaum, V. M. Deuterium Kinetic Isotope Effects in the Gas-Phase S_N2 Reactions of Solvated Fluoride Ions with Methyl Halides. *J. Phys. Chem. A* **2004**, *108*, 9887−9891.
(25) Bartmess, J. E. *Negative Ion Energetics Data in NIST Chemistry WebBook*, NIST Standard Reference Database Number 69; Lindstrom, P. J., Mallard, W. G., Eds.; National Institute of Standards and Technology: Gaithersburg, MD; http://webbook.nist.gov (retrieved Nov 16, 2012),
(26) Van Doren, J. M.; Barlow, S. E.; DePuy, C. H.; Bierbaum, V. M. The Tandem Flowing Afterglow-SIFT-Drift. *Int. J. Mass Spectrom. Ion Process.* **1987**, *81*, 85−100.
(27) Bierbaum, V. M. In *Encyclopedia of Mass Spectrometry*; Gross, M. L., Caprioli, R., Eds.; Elsevier: Amsterdam, The Netherlands, 2003; Vol. *1*, pp 98−109.
(28) Su, T.; Chesnavich, W. J. Parametrization of the Ion-Polar Molecule Collision Rate Constant by Trajectory Calculations. *J. Chem. Phys.* **1982**, *76*, 5183−5185.
(29) Frisch, M. J.; Trucks, G. W.; Schlegel, H. B.; Scuseria, G. E.; Robb, M. A.; Cheeseman, J. R.; Scalmani, G.; Barone, V.; Mennucci, B.; Petersson, G. A. et al. *Gaussian 09*, Revision B.01; Gaussian, Inc.: Wallingford, CT, 2010.
(30) Hierl, P. M.; Ahrens, A. F.; Henchman, M.; Viggiano, A. A.; Paulson, J. F.; Clary, D. C. Nucleophilic Displacement as a Function of Hydration Number and Temperature - Rate Constants and Product Distribution for $OD^-(D_2O)_{0,1,2}$ + CH_3Cl at 200−500 K. *J. Am. Chem. Soc.* **1986**, *108*, 3142−3143.
(31) Viggiano, A. A.; Arnold, S. T.; Morris, R. A.; Ahrens, A. F.; Hierl, P. M. Temperature Dependences of the Rate Constants and Branching Ratios for the Reactions of $OH^-(H_2O)_{(0-4)}$+CH_3Br. *J. Phys. Chem.* **1996**, *100*, 14397−14402.
(32) Seeley, J. V.; Morris, R. A.; Viggiano, A. A. Temperature Dependences of the Rate Constants and Branching Ratios for the Reactions of $F^-(H_2O)_{(0-5)}$ with CH_3Br. *J. Phys. Chem. A* **1997**, *101*, 4598−4601.
(33) Otto, R.; Brox, J.; Trippel, S.; Stei, M.; Best, T.; Wester, R. Single Solvent Molecules Can Affect the Dynamics of Substitution Reactions. *Nat. Chem.* **2012**, *4*, 534−538.
(34) Otto, R.; Brox, J.; Trippel, S.; Stei, M.; Best, T.; Wester, R. Exit Channel Dynamics in a Micro-Hydrated S_N2 Reaction of the Hydroxyl Anion. *J. Phys. Chem. A* **2013**, *117*, 8139−8144.
(35) Baer, T.; Hase, W. L. In *Unimolecular Reaction Dynamics: Theory and Experiment*; Oxford University Press: New York, 1996; pp 1−448.
(36) Jeffrey, G. A. *An Introduction to Hydrogen Bonding*; Oxford University Press: New York, 1997.